70-1022-21

TECHNICAL MEMORANDUM

ATTITUDE CONTROL CAPABILITY FOR PERFORMING THE EARTH RESOURCES EXPERIMENT PROGRAM ON SKYLAB

Bellcomm

36

BELLCOMM, INC.
955 L'ENFANT PLAZA NORTH, S.W., WASHINGTON, D.C. 20024

COVER SHEET FOR TECHNICAL MEMORANDUM

TITLE- Attitude Control Capability for Performing the Earth Resources Experiment Program on Skylab

TM- 70-1022-21

DATE- December 29, 1970

FILING CASE NO(S)- 620

AUTHOR(S)- J. J. Fearnsides

FILING SUBJECT(S) (ASSIGNED BY AUTHOR(S))- Attitude Control
Control Moment Gyros
Earth Resources Experiment Program
Skylab Program

ABSTRACT

This memorandum deals with the capability of the Skylab CMGs to acquire and hold an earth-pointing (Z-LV) attitude. In this attitude experiments in the Earth Resources Experiment Program (EREP) are performed. The results of an MSFC study on this subject are reviewed and used as a point of departure. Included herein are:

1. an operational procedure for obtaining the value of the total CMG angular momentum vector, $\underline{H}$, at an appropriate point in the orbit, that minimizes the amount of TACS propellant consumed in acquiring and holding the Z-LV attitude;

2. an explanation of the way in which this biasing of $\underline{H}$ can be achieved by existing ATMDC software; and

3. some preliminary observations on a method for extending successive orbit capability in the Z-LV attitude with no concomitant increase in TACS propellant consumption.

A comparison of the amount of TACS impulse consumed if $\underline{H}$ is appropriately biased with the impulse required by the MSFC approach is presented in Table 1. All of the results shown are for 120 deg experiment pass regions that are symmetrical with respect to orbital noon.

TACS IMPULSE CONSUMPTION
FOR BIASED AND UNBIASED $\underline{H}$

	$\beta = 0°$	$\beta = 30°$	$\beta = 50°$
UNBIASED $\underline{H}$	20 lb-sec	28 lb-sec	24 lb-sec
BIASED $\underline{H}$	8 lb-sec	8 lb-sec	4 lb-sec

TABLE 1

DISTRIBUTION

COMPLETE MEMORANDUM TO

CORRESPONDENCE FILES

OFFICIAL FILE COPY
plus one white copy for each additional case referenced

TECHNICAL LIBRARY (4)

NASA Headquarters

H. Cohen/MLR
J. H. Disher/MLD
W. B. Evans/MLO
J. P. Field, Jr./MLP
W. H. Hamby/MLO
T. E. Hanes/MLA
A. S. Lyman/MR
M. Savage/MLT
W. C. Schneider/ML

Langley Research Center

P. R. Kurzhals/AMPD

MSC

W. R. Cunningham/CB
R. L. Frost/KS
O. K. Garriott/CB
F. C. Littleton/KM
R. M. Machell/KW
O. G. Smith/KW
H. E. Whitacre/KM

MSFC

W. B. Chubb/S&E-ASTR-SGD
G. B. Hardy/PM-AA-EI
H. F. Kennel/S&E-ASTR-A
G. F. McDonough/S&E-DIR
E. F. Noel/S&E-ASTR-SI
J. W. Sims/S&E-ASTN-PTA
R. G. Smith/PM-SAT-MGR
J. W. Thomas/PM-AA-EI
H. E. Worley/S&E-AERO-DO

COMPLETE MEMORANDUM TO (CONTINUED)

Martin-Marietta

E. F. Bjoro/Washington

Bellcomm

A. P. Boysen
J. P. Downs
D. R. Hagner
W. G. Heffron
D. P. Ling
J. Z. Menard
P. F. Sennewald
J. W. Timko
R. L. Wagner
M. P. Wilson
Departments 2031, 2034 Supervision
Division 101 Supervision
Department 1024 File
Division 102
Central File

The TACS impulse capability is 61,000 lb-sec of which 30,259 lb-sec are allocated for performance of the total mission [2]. Included in this allocation is 100 lb-sec per pass for each of 45 Z-LV passes. The 30,741 pound-seconds of the total capability that is not allocated is a margin for contingencies such as operation with one failed CMG. In view of the results in Table 1 for unbiased $\bar{H}$, 45 Z-LV passes can be performed without biasing and still provide a good margin over what is now allotted. However, the results of Table 1 for biased $\bar{H}$ show that biasing would allow an increase in the number of Z-LV passes (without exceeding any margin requirements) should that be desired. In addition, since the TACS firings in [1] as well as this study occur during the experiment pass, a reduction in the number of firings is beneficial to experiment pointing stability.

BELLCOMM, INC
955 L'ENFANT PLAZA NORTH, S W WASHINGTON, D C. 20024

SUBJECT: Attitude Control Capability for Performing the Earth Resources Experiment Program on Skylab Case 620

DATE: December 29, 1970

FROM: J. J. Fearnsides

TM-70-1022-21

TECHNICAL MEMORANDUM

Introduction

A recent MSFC study [1] explored the possibilities of biasing* the total CMG angular momentum vector, $\underline{H}$, such that the maneuvers associated with the performance of the EREP could be achieved by the nested control law with a minimum expenditure of TACS propellant. The main conclusion was that, while some TACS propellant could be saved by such biasing, not enough could be saved to warrant any increases in ATMDC software complexity. The constraints imposed on the study were:

1. $|\beta| \leq 30°$, and

2. all experiment passes symmetrical about orbital noon. In addition, some preliminary results were given for 2 CMG operation and a statement was made that the spacecraft could recover from a Z-LV pass during the next CMG dump cycle with no TACS expenditure.

The purpose of this memorandum is twofold. First, since [1] contains only results and conclusions, it is felt that a report that explains the procedure and the rationale behind it is necessary. Secondly, since the publication of [1], certain changes in the planned operating procedure of the EREP have been either suggested [2] or made, e.g. the opening of the constraint on the solar incidence angle to $|\beta| \leq 50°$ [3]. The possibility of a more ambitious EREP also suggests a reconsideration of the need for a recipe for biasing $\underline{H}$, especially if it could be accomplished with no increase in the software of the control system. Therefore, some extensions of the results of [1] are also presented which, while not optimal, represent improvements in system performance with no increase in on-board software.

---

*The aptness of this term will become apparent in the sequel.

II. A Z-LV Acquisition and Hold Procedure

Figure 1 illustrates a Z-LV acquisition and hold procedure that has been synthesized from [1] and from the Program Definition Document (PDD) [4]. The goal of this procedure is to maneuver the spacecraft to an earth-pointing attitude in such a way that:

1. experiments may be performed during any 60° segment of the 120° region centered on orbital noon. (The variable γ_3 is employed in Figure 1 to permit consideration of unsymmetrical experiment pass regions);

2. the entire maneuver sequence can be executed by the nested control law rather than requiring TACS only control;

3. the impact on the thermal and power systems is minimal.

A complete description of this procedure requires some preliminary information concerning the momentum sampling strategy contained in the dump maneuver portion of the PDD.* Only those details that are necessary for a logical development are included in this section. Further details are in Appendix A.

The orbital positions designated as (5), (6) and (0) in Figure 1 are related through the characteristics of the sinusoidal component of the gravity-gradient torque, which is the most predominant disturbance on the Skylab spacecraft in the solar inertial attitude. This is most easily seen by considering the case when $\beta=0°$ and when the Y-geometric axis of the spacecraft is parallel to the normal to the orbital plane. For this case the gravity-gradient torque, T_Y, acting along the Y-geometric axis is as shown in Figure 2 where it is plotted versus orbital angular excursion, θ. Using MSFC inertia data [5], the analytical form of the curve in Figure 2 is

$$T_Y(\theta) = -7.085 \sin 2(\theta + \alpha),$$

where $\theta=0$ is defined at orbital noon of the Z-LV pass, and the offset angle, α, is due to the fact that geometric, not

---

*Because the primary spacecraft attitude for Skylab is solar inertial, the momentum dump scheme is designed to work for that attitude. However, as shown in Appendix A, this scheme can be used as well to bias $\underline{H}$ for orbits that include Z-LV passes.

principal, axes are kept aligned with the solar inertial attitude by the control system.* One possible plot of the CMG momentum vector variation due to $T_Y(\theta)$ is shown in Figure 3. The analytical expression corresponding to this plot is now derived.

$$H_Y(t) = H_Y(t_o) - \int_{t_o}^{t} 7.085 \sin 2(\omega_o \tau + \alpha) d\tau,$$

where the fact has been used that $\theta = \omega_o t$, ω_o = the orbital angular rate, and t_o is some initial time. The result of performing the above integration is

$$H_Y(t) = H_Y(t_o) + 3167[\cos 2(\omega_o t + \alpha) - \cos 2(\omega_o t_o + \alpha)]. \quad (1)$$

The plot in Figure 3 corresponds to the selection of

$$H_Y(t_o) = 3167 \cos 2(\omega_o t_o + \alpha). \quad (2)$$

Equations (2) and (1) in combination with the variable changes $\theta = \omega_o t$ and $\theta_o = \omega_o t_o$ lead to (3).

$$H_Y(\theta) = 3167 \cos 2(\theta + \alpha). \quad (3)$$

The adjustment of the level of the curve of $H_Y(\theta)$, e.g. by selecting $H_Y(\theta_o)$ for a given θ_o is called biasing.

Orbital positions (5), (6) and (0) can now be defined. With respect to (3), dump midnight, (6), is located by $(\theta+\alpha) = \pm\pi$. The reason for specifically denoting (6) is that all sampling points in the ATMDC momentum dump strategy are measured relative to (6). Points (5) and (0) are located, respectively, by $\theta+\alpha = -5\pi/4$ and $\theta+\alpha = -3\pi/4$.

---

*The baselined Z-axis rotation, which essentially puts the X-principal axis in the orbital plane, is neglected. Its effect here is very small.

At these points H_Y is equal to its average (or bias) value (in this case, zero*). Note that this is true only if no other torques except T_Y in Figure 2 have acted on the Y axis of the spacecraft and if the spacecraft was in solar inertial for the entire daylight orbit preceeding (5). If the spacecraft were in solar inertial for the orbit preceeding (5) and if a bias momentum were built up during that orbit, then this bias would be evaluated by the sampling strategy and, subsequently, dumped. However, if the spacecraft were not in solar inertial before (5), which is the case for the Z-LV pass, then the solar inertial sampling strategy is not applicable. For this case, the momentum vector is sampled at (5) and the amount that is dumped from (5) to (0) is the amount by which H_Y at (5) differs from the desired bias value [4]. Note that, if this dump is executed exactly, H_Y at (0) is equal to the desired value. In a similar way, when the spacecraft is in solar inertial for the orbit preceeding (5), the level of $H_Y(\theta)$ which determines the value of H_Y at (0), can be established with the existing solar inertial sampling strategy. The details of this procedure comprise the contents of Appendix A. Thus, the importance of (0) is that, since it can be arranged to occur at the end of a dump cycle†, its value can be specified by existing ATMDC software. For this reason it is the starting point for this study as it was for [1].

Orbital position (1) locates the point where the maneuver to acquire the Z-LV attitude is begun [1]. For the $|\beta| \leq 30°$ constraint used in [1], point (0) always occurs during the dark portion of the orbit. Point (1) must be selected some time after effective spacecraft sunrise to allow: correction of any attitude errors that may have accumulated on the dark side, and the updating of the strap-down calculations before beginning the maneuver. The angle γ_1 in Figure 1 was made variable because the duration of the dark portion of the orbit varies with β. For this study, γ_1 was taken to be $\gamma_1(\beta)$ and point (1) taken fixed with respect to effective sunrise. In [1], γ_1 was taken to be constant at the value for $\beta=0°$. This matter is discussed in more detail in §III of this report.

---

*This is also the biasing that was used in [1].

†The regular solar inertial dump cycle is performed over an entire dark side pass rather than over 90 orbital degrees.

The rest of the sequence proceeds in a straightforward manner (See Figure 1). At (2), the acquisition rate is terminated and the orbital rate is initiated. Between (2) and (3) the spacecraft is in the Z-LV attitude. At (3), the orbital rate is terminated and the acquisition rate for the return (to solar inertial) maneuver is initiated. When this rate is terminated at (4), the spacecraft has reacquired solar inertial. It is held in this attitude until (5), when $\underline{H}$ is measured and the gravity-gradient dump maneuver begins.

In [1], the Z-LV maneuvers are symmetrical about orbital noon ($\theta=0$). That is: (2) and (3) are equidistant from $\theta=0$; $\gamma_2 = \gamma_4$, and $\gamma_1 = \gamma_5$. The results of a digital computer simulation of such a symmetrical sequence combined with the biasing of H_Y defined by (2) are shown in Figure 4. In addition, two other runs were made. These are illustrated in Figures 5 and 6 and differ from the run shown in Figure 4 in that the solar incidence angle, β, is taken to be 30° and 50°, respectively.* Note that the component of CMG angular momentum along the Y-geometric axis, not the axis normal to the orbital plane, is the one that is zeroed in the latter two runs. This is because in an orbit with a Z-LV pass, the variation of H_Y (subscript Y denoting the geometric Y axis) exceeds in magnitude the variations of H_X and H_Z, and because the existing ATMDC software can only bias $\underline{H}$ relative to geometric axes. Also, as discussed in §III, the level of projection of $\underline{H}$ onto the geometric X and Z axes, i.e. H_X and H_Z, are also set to zero at (0) as they were in [1]. The TACS impulse expenditure for these three cases is 20 lb-sec, 28 lb-sec and 24 lb-sec, respectively.† These results do not differ significantly from the results of [1].

III. An Operational Procedure for Biasing H_Y for Symmetrical Passes

The momentum profiles in Figures 4 through 6, combined with the existing capability for biasing the level of H_Y (as well

---

*The $\beta=50°$ run, while violating one of the ground rules of [1], is included because of the aforementioned change in the baseline that occurred after the publication of [1].

†The minimum impulse bit used for this study is 4 lb-sec. This number was inferred from section 13 of [4].

as H_X and H_Z), suggest an approach for reducing the amount of TACS propellant consumption even further. Note from these figures that large changes in H_Y occur from (2) to (3). Further, as explained in [6], a substantial component of bias momentum is built up about the axis normal to the orbital plane when the spacecraft is in an Earth-pointing attitude. The sum of these two effects produces the largest change in $\underline{H}$ during the orbit. Thus, if the total change in $\underline{H}$ from (2) to (3) can be centered between the TACS firing thresholds established by the nested control law, then the entire EREP sequence can be executed by the CMGs with no TACS expenditure. This change from (2) to (3) is calculated by adding the following changes.

1. ΔH_Y due to termination of maneuver rate.

$$\Delta H_{Y21} = (I\underline{\omega}_1)\cdot\underline{a}_Y \text{ ft-lb-sec}, \tag{4}$$

where: I = inertia matrix, slug-ft^2,

$\underline{\omega}_1$ = acquisition rate, (sec)$^{-1}$, for the eigenaxis maneuver from solar inertial to Z-LV,*

$\underline{a}_Y$ = unit vector along the positive Y-axis of the spacecraft.

2. ΔH_Y due to initiation of orbital rate.

$$\Delta H_{Y22} = -(I\underline{\omega}_o)\cdot\underline{a}_Y \text{ ft-lb-sec},$$

where: $\underline{\omega}_o$ = orbital angular rate, (sec)$^{-1}$.

3. ΔH_Y due to bias momentum accumulation in Z-LV attitude.

$$\Delta H_{Y23} = 3\omega_o{}^2 I_{XZ}\Delta t \text{ ft-lb-sec}.$$

where I_{XZ} = the 1, 3 element of the inertia matrix in slug-ft^2, and

Δt = the total time spent in Z-LV attitude.

For β=0° and an Experiment Pass Region (EPR) defined by γ_3 = 120° (See Figure 1), this total change exceeds the range permitted by the nested strategy for no TACS firing.

---

*In spacecraft coordinates, $\underline{\omega}_1 = [0\ -\omega_1\ 0]$. That is $\underline{\omega}_1$ is positive about the -Y geometric axis.

However, some propellant can still be saved by positioning (2) in Figures 4 through 6 as closely as possible to the TACS firing threshold.* Therefore, whether or not any TACS firing will be required, it is possible by simple calculation to obtain a desired value for H_Y just before the termination of the EREP acquisition maneuver rate. This value, in turn, corresponds to a unique value of H_Y at (0), which can be established in three steps.

1. Integrate the Y component of $\dot{\underline{H}}$ in equation (5) in reverse time from (2) to (1).

$$\dot{\underline{H}} + \underline{\omega}_1 \times \underline{H} = \underline{T}_{gm} - \underline{\omega}_1 \times I\underline{\omega}_1 \tag{5}$$

where: $\underline{\omega}_1$ is the vector representation, in spacecraft coordinates, of the maneuver rate and $\underline{T}_{gm}$ is the analytical representation of the gravity-gradient torque during the acquisition maneuver.

2. Calculate the change in H_Y required to initiate the acquisition rate and subtract it from the final value of the previous integration. That is, if $H_Y\ (t_1+)$ defines the desired value of momentum immediately after acquisition of the maneuver rate, and $H_Y\ (t_1-)$ is the value of momentum immediately before this rate acquisition, then

$$H_Y\ (t_1-) = H_Y\ (t_1+) + \Delta H_{Y21}$$

where ΔH_{Y21} is defined by (4).

3. Integrate (6) in reverse time from (1) to (0).

$$\dot{H}_Y = T_{YS} \tag{6}$$

where T_{YS} is the Y component of the gravity-gradient torque in the solar inertial attitude. The value of H_Y calculated by the

---

*The threshold used for this study was 6412.5 ft-lb-sec. This was calculated using a conservative value of 2250 ft-lb-sec for the individual CMG angular momentum (with the new wheel speed) in the equation, $H_{max}=(.95)(3)(2250) = 6412.5$ ft-lb-sec.

latter integration is the desired value of H_Y at ⓪ . As previously mentioned, a description of how this value can be achieved with existing ATMDC software is explained in Appendix A.

Note that there is no need to perform the above calculations on-board. The desired value of H_Y at ⓪ could be calculated on the ground and up-linked 4 or 5 orbits* before the scheduled Z-LV acquisition orbit.

The above procedure cannot be extended in a simple way to establish optimal values for H_X and H_Z. This is because these axes are rotating relative to an inertial coordinate system** during various segments of the orbit described in Figure 1. Thus, no single value of H_X and H_Z can be chosen to minimize the magnitudes of their variation. However, very little performance penalty accrues from not biasing H_X and H_Z since their variations are much smaller than the variation of H_Y. For the computer runs performed in this study, H_X and H_Z were set to zero at ⓪ and produced good results.

The result of applying this procedure to a case that is similar to the one shown in Figure 4 i.e. a 120° symmetrical experiment pass region and $\beta = 0°$, is $H_Y(\theta_o) =$ 390 ft-lb-sec. The momentum profile that obtains is plotted in Figure 7. The TACS impulse expenditure for this case is 8 lb-sec as opposed to the 20 lb-sec expended if $H_Y(\theta_o) = 0$. Figures 8 and 9 show the resulting momentum profile for the same γ_3 and $H_Y(\theta_o) = 390$ ft-lb-sec, except that $\beta = 30°$ and 50°, respectively, for these two cases. The corresponding TACS impulse expenditures are 8 lb-sec and 4 lb-sec corresponding respectively to 28 lb-sec and 24 lb-sec expended when $H_Y(\theta_o) = 0$ (Figures 5 and 6). Note that even better results could have been obtained for $\beta \neq 0$ cases if a new evaluation of the reverse integration had been made rather than using the desired value for $\beta = 0$ case.

---

* This number, a result of simulations run at MSFC, was obtained on a telephone conversation with H. F. Kennel on November 30, 1970.

**An exposition of the variation of $\underline{H}$ in a rotating spacecraft is given in [6].

Actually, the plots in Figures 7 through 9 differ slightly from their counterparts in Figures 4 through 6 in two additional ways. Namely, they use variable values of γ_1 and γ_4 in Figure 1. These modifications, discussed below, could be added to any ground-based computation of the desired value of H_Y at (0) .

The variability of γ_1 is possible because of the variation of the duration of the dark portion of the orbit with β. If the dark portion of the orbit is greater than 90 orbital degrees, which insures completion of a dump maneuver, then (1) can be selected with respect to effective spacecraft sunrise. This allows a longer maneuver time for cases when $|\beta| > 0$. For this study, (1) occurs approximately one orbital degree after effective sunrise.

The variability of γ_4 can be used to provide an additional CMG momentum dump capability about the Y-geometric axis. That this capability may be of some importance is seen by noting that the value of H_Y at (5) in Figure 4 is approximately -1500 ft-lb-sec. Moreover, this quantity was calculated by considering only the effects of the gravity-gradient torque. If the aerodynamic and venting torques were included, (the latter having a relatively large effect on the Y-axis) H_Y could be increased substantially. Depending on the size of the increase, H_Y could achieve a value that could not be dumped simultaneously with the X and Z axis momentum dump requirements. The details of a procedure for providing extra Y-axis dump capability are given in Appendix B.

IV. Biasing for Unsymmetrical Passes

As mentioned in §II, the nested control system must have the capability to permit performance of the EREP experiments during some 60° segment of the symmetrical region defined by $\gamma_3 = 120°$ in Figure 1. Thus, it is possible to produce passes that are not symmetrical with respect to orbital noon. The most unsymmetrical passes are:

1. when (2) is 60° before orbital noon and (3) is coincident with orbital noon.

2. when (2) is coincident with orbital noon and (3) occurs 60° later. The first of these two cases will be called the noon exit case and the latter the noon acquisition case.

As shown in Figure 10, the noon exit case can be handled by the same procedure used for symmetrical passes with an added 8 lb-sec/orbit impulse penalty (16 lb-sec total). If H_Y is zeroed at (0), the impulse expenditure is 24 lb-sec. Either of these may be considered acceptable. However, the setting of H_Y to zero at (0) for the noon acquisition, $\beta = 0°$ case results in a 44 lb-sec TACS impulse expenditure (see Figure 11). Further, not much improvement occurs if H_Y at (0) = 390 ft-lb-sec. Thus, some generalization of the procedure is necessary if unsymmetrical passes are to be considered. This is done as follows

1. Determine $\Delta H_Y(t_2) = \Delta H_{Y21} + \Delta H_{Y22}$ at (2) as in §III.

2. Determine $\Delta H_Y(t_3) = \Delta H_Y$ at (3) as follows:

a. ΔH_Y due to termination of orbital rate

$$\Delta H_{Y31} = (I\underline{\omega}_o)\cdot\underline{a}_Y \text{ ft-lb-sec} = -\Delta H_{Y22}.$$

b. ΔH_Y due to initiation of return maneuver rate

$$\Delta H_{Y32} = (I\underline{\omega}_2)\cdot\underline{a}_Y \text{ ft-lb-sec},$$

where $\underline{\omega}_2$ = the vector representation in spacecraft coordinates of the return maneuver rate.

3. If $|\Delta H_Y(t_3)| \leq |\Delta H_Y(t_2)|$, use the symmetrical procedure in §III. That is, calculate ΔH_Y from (2) to (3) and center, integrate (5) in reverse time, calculate ΔH_{Y21}, and integrate (6) in reverse time.

4. If $|\Delta H_Y(t_3)| > |\Delta H_Y(t_2)|$, proceed to 5.

5. Center $\Delta H_Y(t_3)$ with respect to the thresholds established by the nested control system strategy. The greatest lower bound of the centered profile provides the boundary value for the following integration.

6. Perform a reverse time integration on the equation,

$$\dot{\underline{H}} + \underline{\omega}_o \times \underline{H} = \underline{T}_{g_E} - \underline{\omega}_o \times I\underline{\omega}_o,$$

where $\underline{T}_{gE}$ = the gravity-gradient torque acting on the Earth-pointing spacecraft. This integration is carried out from (3) to (2) (see e.g., Figure 11).

7. Algebraically add the negative of $\Delta H_Y(t_2)$ to the final value of the integration performed in 6.

8. Continue as with the symmetrical procedure, i.e. integrate in reverse time from (2) to (1), calculate $\Delta H_Y(t_1)$ and add it appropriately to the final value of the previous integration, and then integrate in reverse time from (1) to (0).

When the noon acquisition, $\beta = 0°$ case was run with the value of H_Y at (0) specified by the above calculation (i.e., -2610 ft-lb-sec)†, the TACS impulse expenditure was reduced from 44 lb-sec to zero lb-sec (see Figure 12).

V. Conclusions

While the results of [1] are adequate within the framework of their groundrules, i.e., symmetrical Z-LV passes and $|\beta| \leq 30°$, the possibility of a more ambitious EREP warrants the development of an operational technique for biasing $\underline{H}$. The approach taken in this memorandum was to extend the results of [1] without trying to change the baselined maneuver sequence.* Three extensions to the results in [1] were obtained:

1. An operational procedure was given for determining a value of $H_Y(\theta_o)$ that reduces the TACS expenditure for symmetrical Z-LV passes.

2. An extension of the above procedure for unsymmetrical maneuvers was developed.

3. Some observations were made in Appendix B on providing extra dump capability for the purpose of extending the number of successive Z-LV passes that can be made without increasing TACS expenditure.

Finally, it should be mentioned that the above operational procedure for determining $H_Y(\theta_o)$ is of limited value if only two CMGs are operative. In such a case recourse might be made to the maneuver sequences described in [6] for substantial reduction of TACS expenditure.

---

*An analysis of other possible maneuver sequences was presented in [6].

†This depends on the ability of the CMGs to hold the spacecraft in solar inertial with, say, a 1305 ft-lb-sec bias and no TACS firings. This seems reasonable.

Acknowledgement

The computer simulation of the variation of $\underline{H}$ in various attitude modes and subjected to the influences of gravity-gradient torque and the TACS (through the nested control law), was programmed by P. R. Dowling. Her assistance during this project was most valuable and is gratefully acknowledged. I would also like to thank W. Levidow for helpful discussions on the CMG momentum dump strategy and R. W. Grutzner for providing a quick numerical solution to the transcendental equation in Appendix B.

J. J. Fearnsides

1022-JJF-mef

Attachments

REFERENCES

1. "Investigation of CMG Capability to Maneuver and Control Skylab A in 'Z-Local Vertical' for Earth Resources Experiments," S&E-ASTR-SG-61-70, MSFC, June 18, 1970.

2. DeGraaf, D. A., "Trip Report - Mission Requirements Panel Meeting at MSC - Case 610," Bellcomm Memorandum for File, B70 09051, September 18, 1970.

3. Minutes of the Twentieth Skylab Mission Requirements Panel, S&E-CSE-A-70-294, MSFC, June 9, 1970.

4. Apollo Telescope Mount Digital Computer (ATMDC) Program Definition Document (PDD), Part I, MSFC-DRL-008A, IBM No. 70-207-0002, Prepared for MSFC by IBM Space Systems Center, Huntsville, Ala., November 4, 1970.

5. S&E-ASTN-SAE Program WP97B, MSFC, October 7, 1970.

6. Fearnsides, J. J., "A Study of Some Attitude and Control Options Compatible with the Performance of Earth-Pointing Experiments by the AAP Cluster," Bellcomm Technical Memorandum, TM-70-1022-2, February 3, 1970.

APPENDIX A

SOME DETAILS ON THE SAMPLING TECHNIQUES OF THE CMG MOMENTUM DUMP SCHEME

The reason for initializing the $\underline{H}$ vector at orbital position (0) is imbedded in the details of how the CMG momentum is sampled at various points in the orbit. This sampling is performed for the purpose of determining how much CMG momentum should be dumped during the succeeding night-time pass. A complete description of the momentum dump scheme is given in Section 10 of [5]. The only aspects of that scheme that are presented here are those necessary for a description of how the ATMDC software would command the $\underline{H}$ vector to be positioned properly at (0) .

A general mathematical representation of the CMG momentum variation along the body axes is

$$H_i(\theta) = H_{0i} + H_{1i}(\theta+\alpha_i-3\pi/4) + H_{2i}\cos 2(\theta+\alpha_i) \quad , \qquad (A\text{-}1)$$

where: $\theta = \omega_0 t$ = the orbital angular excursion measured from orbital noon, α_i = the aforementioned angular offset due to the non-parallel relationship between principal and geometric axes, $i = x,y,z$, H_{ji} = constants and $j = 0,1,2$. Note that the momentum variation is comprised of a constant term, a term that increases linearly with time or orbital angle relative to (0) , and a sinusoidally varying term. The constant term, H_{0i}, establishes the CMG momentum level and is the quantity that can be adjusted by the dump regime. As previously mentioned, the following definitions can be made:

1. dump midnight, (6) , is defined by

$$\theta + \alpha = \pm m\pi, \quad m = 1,3,5,\ldots \quad ,$$

2. dump noon is defined by $\theta + \alpha = 0$,*

3. $H_k(n)$ is the value of H_Y measured at a point $k\pi/4$ from dump midnight, $k = 2,3,4,5,6,7$, during the $n^{\underline{th}}$ consecutive orbit containing a Z-LV pass, $n = 1,2,\ldots$.

To complete the preliminaries, the assumption will be made that $H_{1Y} = 0$ in (A-1). This assumption is nominally true because of the Z-axis rotation that is selected to minimize the bias momentum accumulation about the Y and Z axes of the spacecraft. The Y-axis momentum variation will, then, be described by

$$H(\theta+\alpha) = H_0 + H_2\cos 2(\theta+\alpha) \quad . \tag{A-2}$$

Note that the Y subscripts have been dropped.

The ATMDC equations for the amount of momentum to be dumped to achieve a certain level for $\underline{H}(\theta)$ is given by (A-3). In this equation

$$H_A(n) = \tfrac{1}{2}[H_3(n) + H_5(n)] - H_B \tag{A-3}$$

$$H_0(n+1) = H_0(n) - H_A(n) \quad . \tag{A-4}$$

H_B is an input that corresponds to the desired level of the momentum variation and to the desired value of H_Y at ⓓ . The connection between the level and $H_Y(\theta_0)$ will be shown in the next paragraph. Equation (A-4) expresses the fact that the level of H_Y (i.e., H_0) during the n + first orbit equals the level of H_Y during the $n^{\underline{th}}$ orbit less the amount dumped during

---

*The $\alpha_i = \alpha_1(\beta)$ are slightly different for each axis. We use here and from now on $\alpha = \alpha_Y$ since the initialization procedure is not performed for the X and Z axes.

the $n^{\underline{th}}$ dump cycle. This assumes that the actual dumped momentum is equal to the commanded dump momentum.

The sampling instants in (A-3), i.e., k = 3,5, have been chosen to remove the effect of the sinusoidally varying term in (A-2). To show this, note that,

$$H_3(n) = H_0(n) + H_2(n)\cos 2(-\pi/4) = H_0(n)$$

$$H_5(n) = H_0(n) + H_2(n)\cos 2(\pi/4) = H_0(n)$$

which when substituted into (A-3) yields

$$H_A(n) = H_0(n) - H_B \quad . \tag{A-5}$$

(A-5) yields the amount of H_Y to be dumped for the purpose of establishing a new level*. The value of this new level is established by (A-4),

$$H_0(n+1) = H_0(n) - H_A(n) = H_0(n) - H_0(n) + H_B = H_B \quad . \tag{A-6}$$

Note that this level will be maintained until a desired value other than H_B is inputted. This is shown by solving (A-3) and (A-4) for $H_A(n+1)$ and $H_0(n+2)$.

$$H_A(n+1) = H_0(n+1) - H_B = 0$$

$$H_0(n+2) = H_0(n+1) - H_A(n+1) = H_B$$

---

*This momentum has been separated from the momentum that will be dumped, e.g., about the X-axis, due to such terms in (A-1) as $H_{1X} \neq 0$.

Finally, it is easy to show that H_Y at ⓪ of the n + first orbit after n orbits in solar inertial is equal to H_B. To do this, note that ⓪ corresponds to $(\theta+\alpha) = -3\pi/4$. Thus, (A-2) becomes

$$H(n+1) = H_0(n+1) + H_2\cos(-3\pi/2) ,$$

$$= H_B .$$

If $H_{1Y} \neq 0$ in (A-1), a digital filter equation [5] governs the convergence of H_Y to its desired level. This level will not, in general, be reached after a single dump cycle. Therefore, as mentioned in §III, the off-line calculation of H_B should be up-linked 4-5 orbits before the schedule Z-LV pass to allow enough time for the system to readjust the momentum level.

APPENDIX B

AN ADDITIONAL Y-AXIS GRAVITY-GRADIENT DUMP CAPABILITY

As mentioned in §III, an extension of the presently baselined maximum of two successive Z-LV passes raises the question of whether or not the momentum dump cycle can achieve successively new values of H_Y at ⓪ . Were this to occur, the desired value of H_Y at ⓪ could not be attained and more than the minimum amount of TACS propellant would be consumed. The purpose of this Appendix is to show how to deal with this situation by varying γ_4 (see Figure 1) to provide an additional Y-axis gravity-gradient dump capability.

B-1 A General Description of the Procedure

Consider once again, the momentum profile in Figure 4. Note that, for a symmetrical pass, the momentum variation would be symmetrical were it not for the bias term and the TACS firings that occur during the Z-LV attitude hold segment. This asymmetry can be (partially or totally) compensated for by making $\gamma_4 < \gamma_2$ (see Figure 1). A heuristic explanation of this statement is based on two principles:

P1. the sinusoidal variation of the gravity-gradient torque as shown in Figure 2, and

P2. the inverse relationship between the momentum variation due to the gravity-gradient torque and the rate of rotation relative to a set of local vertical coordinates.*

It is also helpful to note that, during both the acquisition and the return maneuvers, the spacecraft moves at a rate $\omega > \omega_0$ relative to local vertical coordinates.

Refer to Figure 1. From ⓪ to ① the spacecraft is in solar inertial and, for the case shown, is always in a region of negative gravity-gradient torque about the Y-axis. Similarly, from ④ to ⑤ , the spacecraft is in solar inertial and, for the case shown, always in a region of positive gravity-gradient torque about the Y-axis. If $\gamma_1 = \gamma_5$, the net change in H_Y over

---

*An example of P2 is given in §B-2 of this Appendix.

these two segments is zero. In the same fashion, a look at Figure 4 shows that there is a net positive change from (1) to (2) (neglecting that ΔH_Y for maneuver acquisition) and a corresponding negative change from (3) to (4) (also neglecting ΔH_Y for maneuvers). Since the bias accumulation is negative, from (2) to (3), it would be advantageous if the net positive ΔH_Y on the afternoon side of the orbit exceeded the net negative change on the forenoon side. That this can be accomplished by setting $\gamma_4 < \gamma_2$ (and therefore, $\gamma_5 > \gamma_1$) is a direct result of P_1 and P_2. The mathematical statement of this procedure is

$$\delta H_{01} + \delta H_{12} + \delta H_{34} + \delta H_{45} > 0 \quad ,$$

where $\delta H_{ij} = H_j - H_i$. Whether or not this increase in H_Y is enough to offset the negative accumulation during the Z-LV pass depends on the existence of a solution for γ_4 in (B-1) that does not violate momentum constraints.

$$\delta H_{01} + \delta H_{12} + \delta H_{23} + \delta H_f + \delta H_{34} + \delta H_{45} = 0 \qquad \text{(B-1)}$$

where δH_f = the amount of momentum put into (or taken out of) the system by TACS firings.

There are three points to be noted about (B-1)

1. It does not take into account the ΔH_Y's necessary for the acquisition and removal of various maneuver rates. This is because, if no TACS assist is used for these functions, they cancel each other. In a case such as the one shown in Figure 11, (B-1) would have to be modified to include these ΔH_Y's.

2. The determination of γ_4 in (B-1) represents a solution to a transcendental equation and must, therefore, be done numerically. An example of a calculation of the solution to (B-1) for a particular case is given in §B-2 of this Appendix.

3. If the solution of (B-1) implies a rate that violates momentum constraints, then one of two options could be used.

a. The γ_4 that corresponds to the largest allowable ΔH_Y for maneuver acquisition could be used. This was done for the run illustrated by Figure 7 and produces an effective dump of 600 ft-lb-sec. Note the improvement relative to Figure 4.

b. Another angle, say γ_3, could also be made variable. While this makes (B-1) a single equation with two unknowns, it might be possible to incorporate a constraint equation, e.g., the momentum constraint, for the purpose of achieving a unique solution.

B-2 An Example

In §B-1, a description of a procedure for providing additional Y-axis dump capability was presented. The calculation to be made was expressed by a functional equation (B-1), which is repeated below for convenience. The purpose of this section is to provide an example of the type of calculation required to solve (B-1).

$$\delta H_{01} + \delta H_{12} + \delta H_{23} + \delta H_f + \delta H_{34} + \delta H_{45} = 0 \qquad \text{(B-1)}$$

where $\delta H_{ij} = H_j - H_i = H(\ j\ ) - H(\ i\ )$, $i = 0,1,2,3,4$; $j = i+1$.

The solution of (B-1) will be calculated for the run that is illustrated in Figure 7. Since γ_4 is the only variable, the first four terms of (B-1) are constant. The functional forms corresponding to these terms are easily determined and will be omitted. From Figure 7,

$$\delta H_{01} = H_1 - H_0 = -2321 - 390 = -2711$$

$$\delta H_{12} = H_2 - H_1 = 6399 - 3744 = 2655$$

$$\delta H_f + \delta H_{23} = H_3 - H_2 = -6408 + 4806 = -1602$$

$$\therefore\ \delta H_{34} + \delta H_{45} = 1658 = -\delta H_{01} - \delta H_{12} - \delta H_{23} - \delta H_f \qquad \text{(B-2)}$$

The functional form of δH_{34} is determined as follows. If t_3 and t_4 are the respective times corresponding to (3) and (4), then, for a spacecraft maneuvering at a rate ω_2 relative to solar inertial,

$$\delta H_{34} = H_4 - H_3 = \int_{t_3}^{t_4} T_{gr}(t)dt \qquad \text{(B-3)}$$

where T_{gr} = the Y-axis component of the gravity-gradient torque. This can be shown to be equivalent to

$$\delta H_{34} = \frac{7.085}{2(\omega_0+\omega_2)}\{\cos 2[(\omega_0+\omega_2)(t_4-t_3)+\alpha] - \cos 2\alpha\}. \qquad \text{(B-4)}$$

The unknown quantities in (B-4) are t_4 and ω_2. However, these quantities are related by

$$\omega_2(t_4 - t_3) = \omega_0 t_3 \quad . \qquad \text{(B-5)}$$

Substituting (B-5) into (B-4), letting $\theta_4 = \omega_0 t_4$ and $\theta_3 = \omega_0 t_3$, and using $\omega_0 = 1.11845 \times 10^{-3}(\text{sec})^{-1}$, finally leads to

$$\delta H_{34} = 3167.3 \frac{(\theta_4-\theta_3)}{\theta_3}\{\cos 2(\theta_4 + \alpha) - \cos 2\alpha\} \qquad \text{(B-6)}$$

where θ_4 is the only unknown.

From (4) to (5) the spacecraft is in the solar inertial attitude. The gravity-gradient torque for this mode is illustrated in Figure 2 and is given by

$$T_Y = -7.085 \sin 2(\omega_0 t + \alpha).$$

Therefore,

$$\delta H_{45} = \frac{7.085}{2\omega_0} \{\cos 2(\omega_0 t_5 + \alpha) - \cos 2(\omega_0 t_4 + \alpha)\}^* . \qquad \text{(B-7)}$$

For this example, $\omega_0 t_5 + \alpha = 3\pi/4$. This implies that

$$\delta H_{45} = -3167.3 \cos 2(\theta_4 + \alpha) . \qquad \text{(B-8)}$$

The substitution of (B-6) and (B-8) into (B-2) yields a transcendental equation that must be solved numerically. For this example, the solution of (B-2) violated the momentum constraints on the system imposed by the nested control strategy. The alternatives for this case were discussed in §B-1.

---

*The terms outside the curly brackets in (B-4) and (B-7) illustrate P2 in §V.

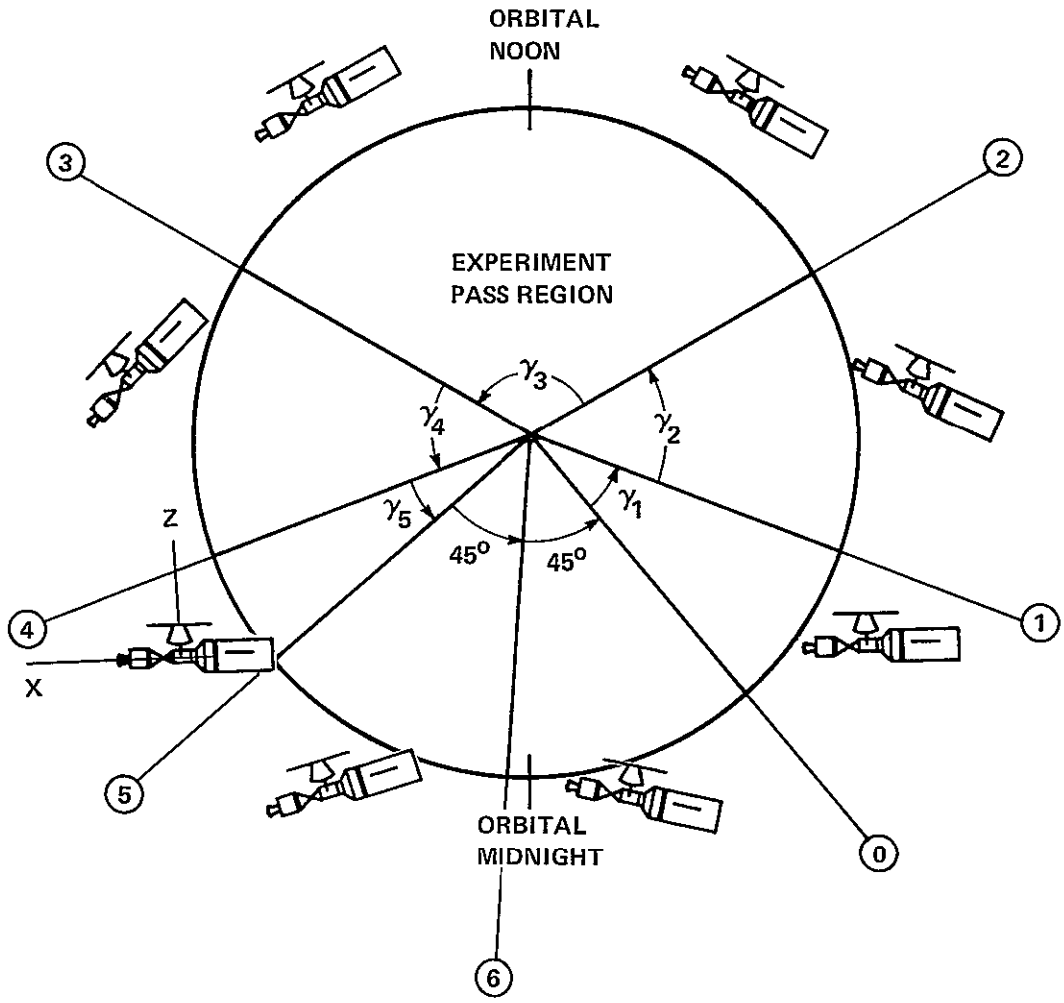

⑥ ORBITAL POSITION OF " DUMP MIDNIGHT".

ATTITUDE PROFILE

FROM:

⑤ TO ⓪ , SPACECRAFT EXECUTES DUMP MANEUVER.
⓪ TO ① , SPACECRAFT HELD IN SOLAR INERTIAL ATTITUDE.
① TO ② , SPACECRAFT MANEUVERS TO Z-LV ATTITUDE.
② TO ③ , SPACECRAFT HELD IN Z-LV ATTITUDE
③ TO ④ , SPACECRAFT MANEUVERS BACK TO SOLAR INERTIAL ATTITUDE.
④ TO ⑤ , SPACECRAFT HELD IN SOLAR INERTIAL ATTITUDE
⑤ TO ⓪ , SPACECRAFT EXECUTES DUMP MANEUVER.

FIGURE 1 - PROCEDURE FOR ACQUISITION AND HOLD OF Z-LV ATTITUDE

B-7

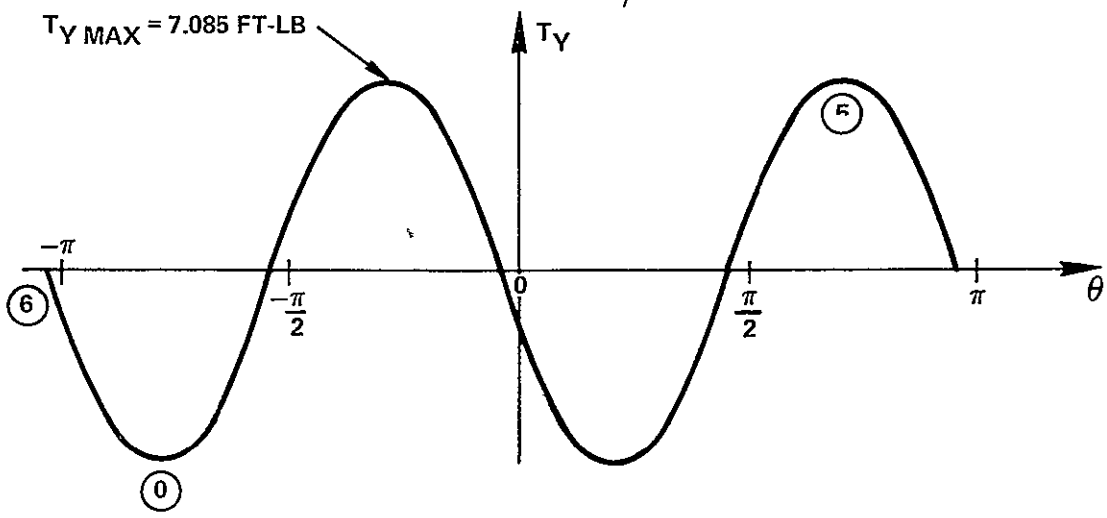

T_Y - component of gravity-gradient torque acting about the Y geometric axis when it is parallel to the normal to the orbital plane.

θ - orbital excursion angle, $\theta = 0$ corresponds to orbital noon, $\theta = \pm\pi$ corresponds to orbital midnight.

FIGURE 2 - GRAVITY-GRADIENT TORQUE VS ORBITAL EXCURSION

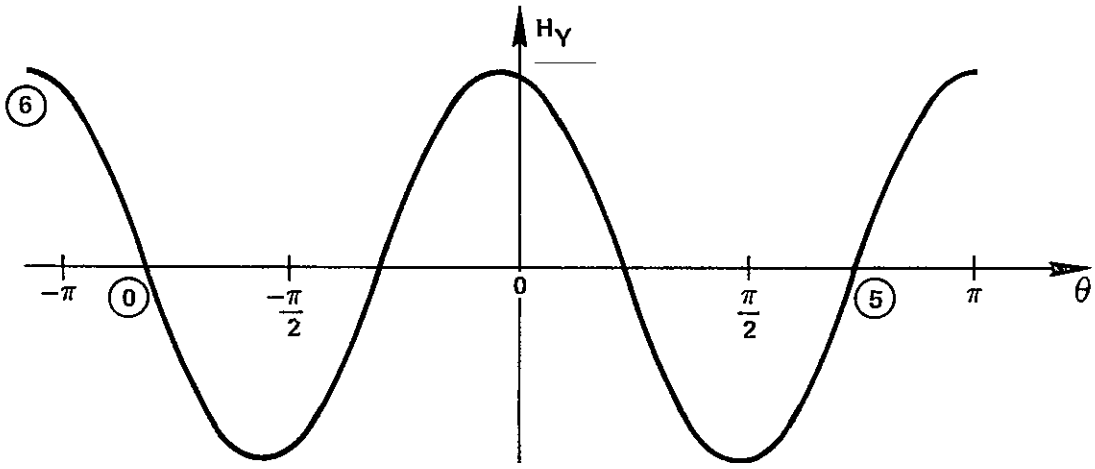

H_Y - MOMENTUM VARIATION PRODUCED BY T_Y IN FIG. 2

FIGURE 3 - CMG ANGULAR MOMENTUM VS ORBITAL EXCURSION

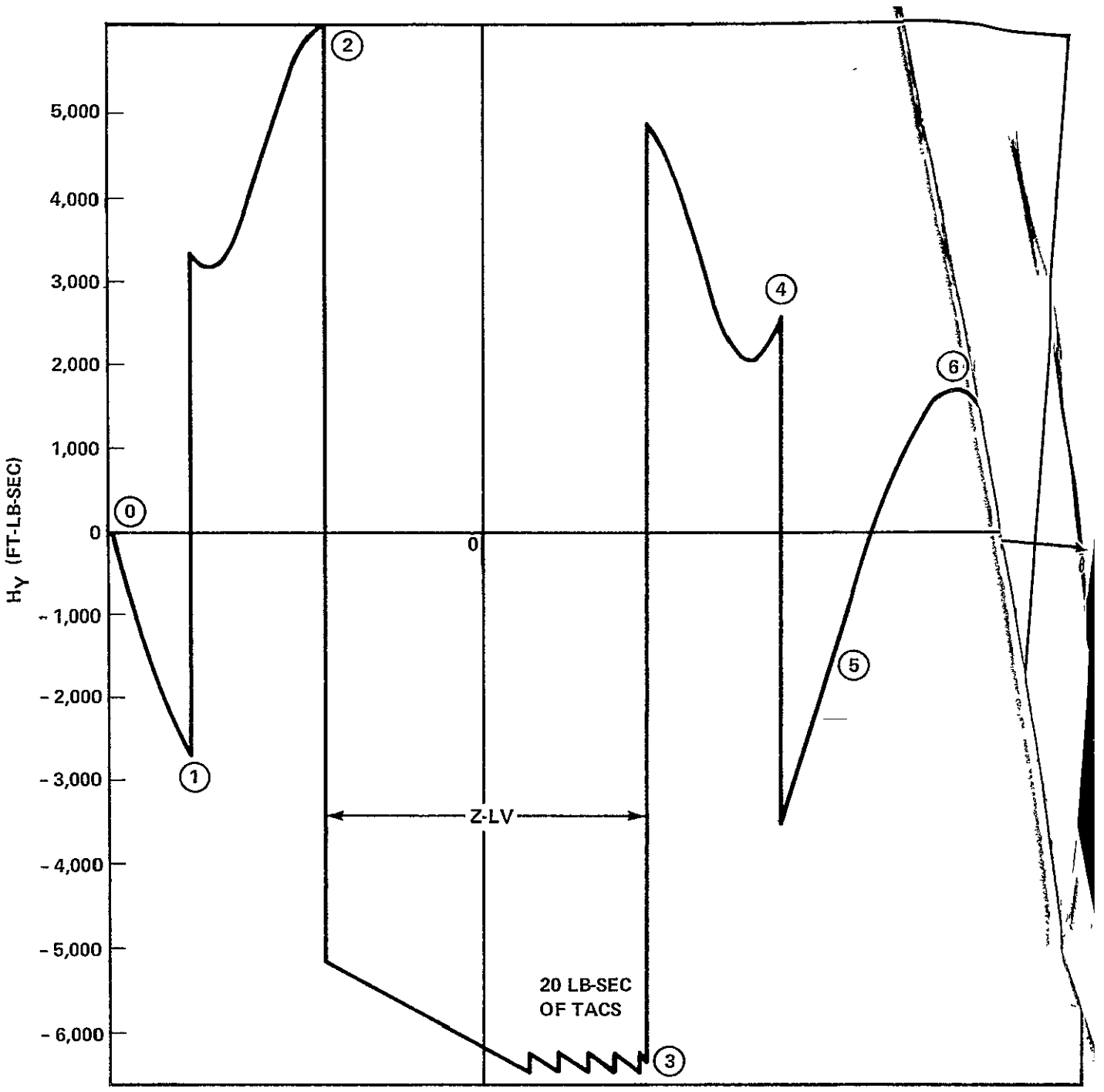

FIGURE 4 – Y-AXIS COMPONENT OF $\underline{H}$ VS ORBITAL ANGULAR EXCURSION, θ.

120° SYMMETRICAL Z-LV PASS, $\beta = 0°$
$\underline{H}'(0) = [\,0\ 0\ 0\,] = \underline{H}'(\theta_0)$, 2250 FT-LB-SEC PER CMG
SPACECRAFT IN SOLAR INERTIAL FROM (5) TO (0)

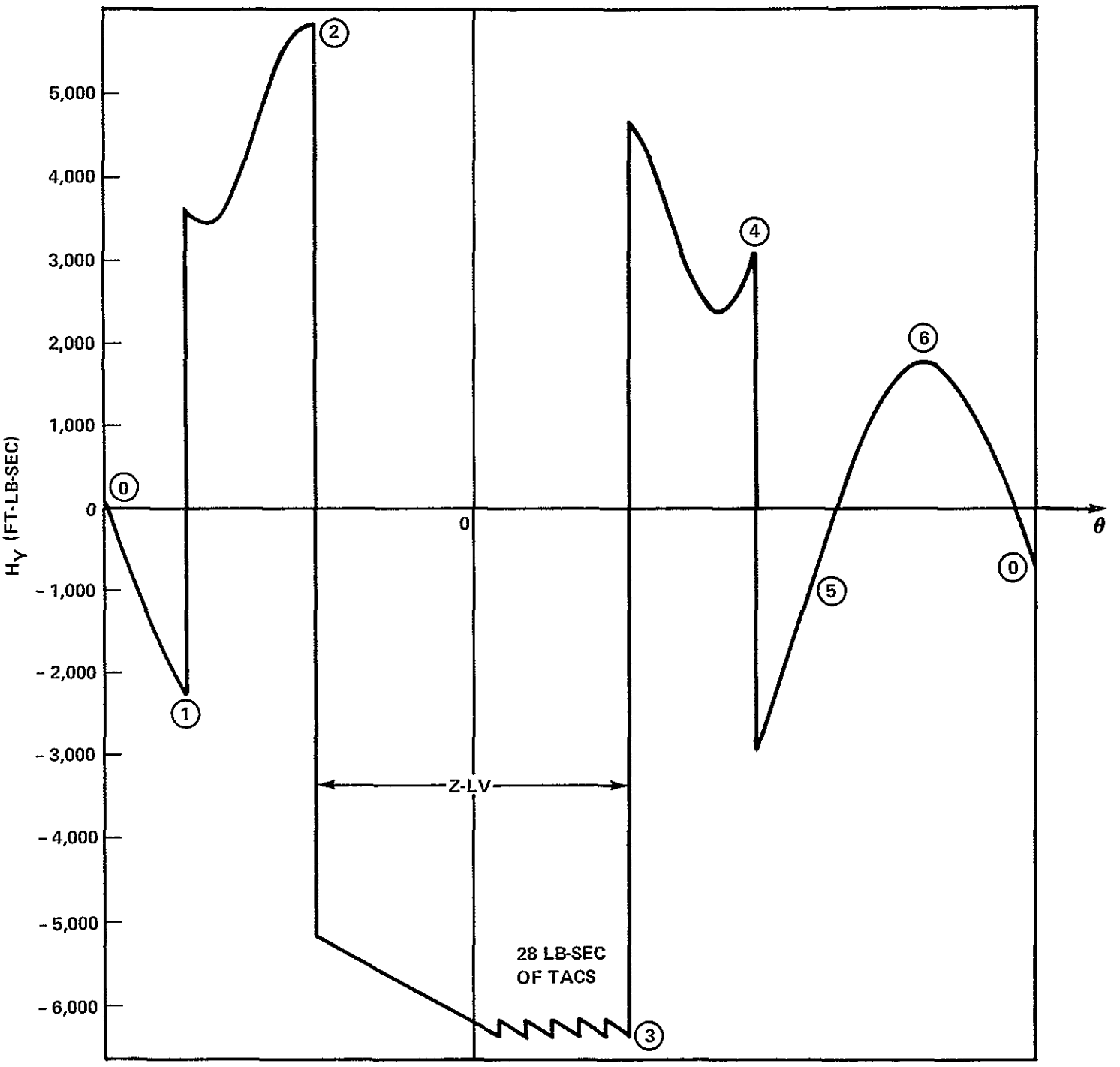

FIGURE 5 - Y-AXIS COMPONENT OF $\underline{H}$ VS ORBITAL ANGULAR EXCURSION, θ.

120° SYMMETRICAL Z-LV PASS, $\beta = 30°$

$\underline{H}'$ (0) = [0 0 0] = $\underline{H}'(\theta_0)$, 2250 FT-LB-SEC PER CMG

SPACECRAFT IN SOLAR INERTIAL FROM (5) TO (0)

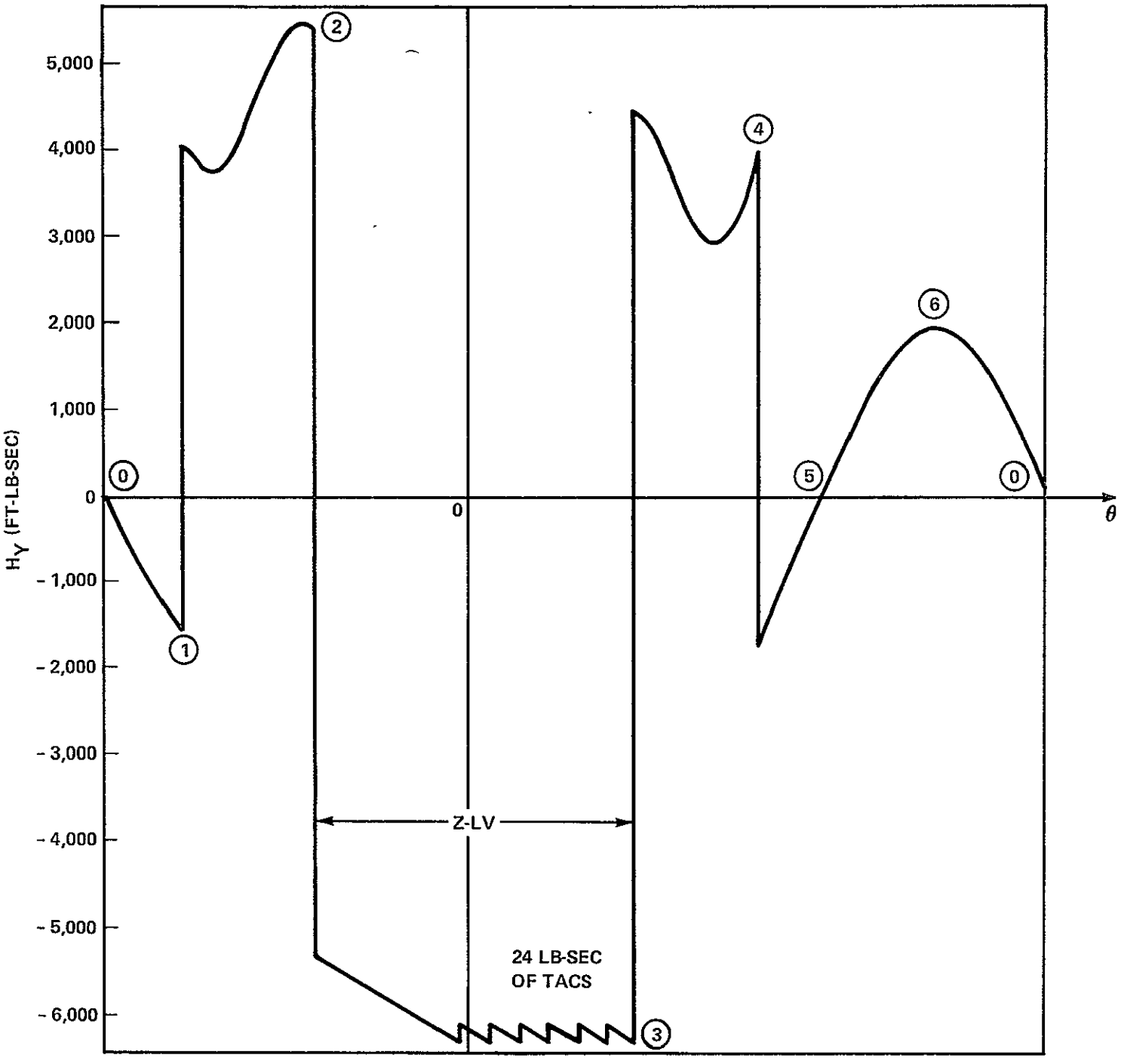

FIGURE 6 - Y-AXIS COMPONENT OF $\underline{H}$ VS ORBITAL ANGULAR EXCURSION

120° SYMMETRICAL Z-LV PASS, $\beta = 50°$

$\underline{H}'$ (0) = [0 0 0] = $\underline{H}'$ (θ_0), 2250 FT-LB-SEC PER CMG

SPACECRAFT IN SOLAR INERTIAL FROM (5) TO (0)

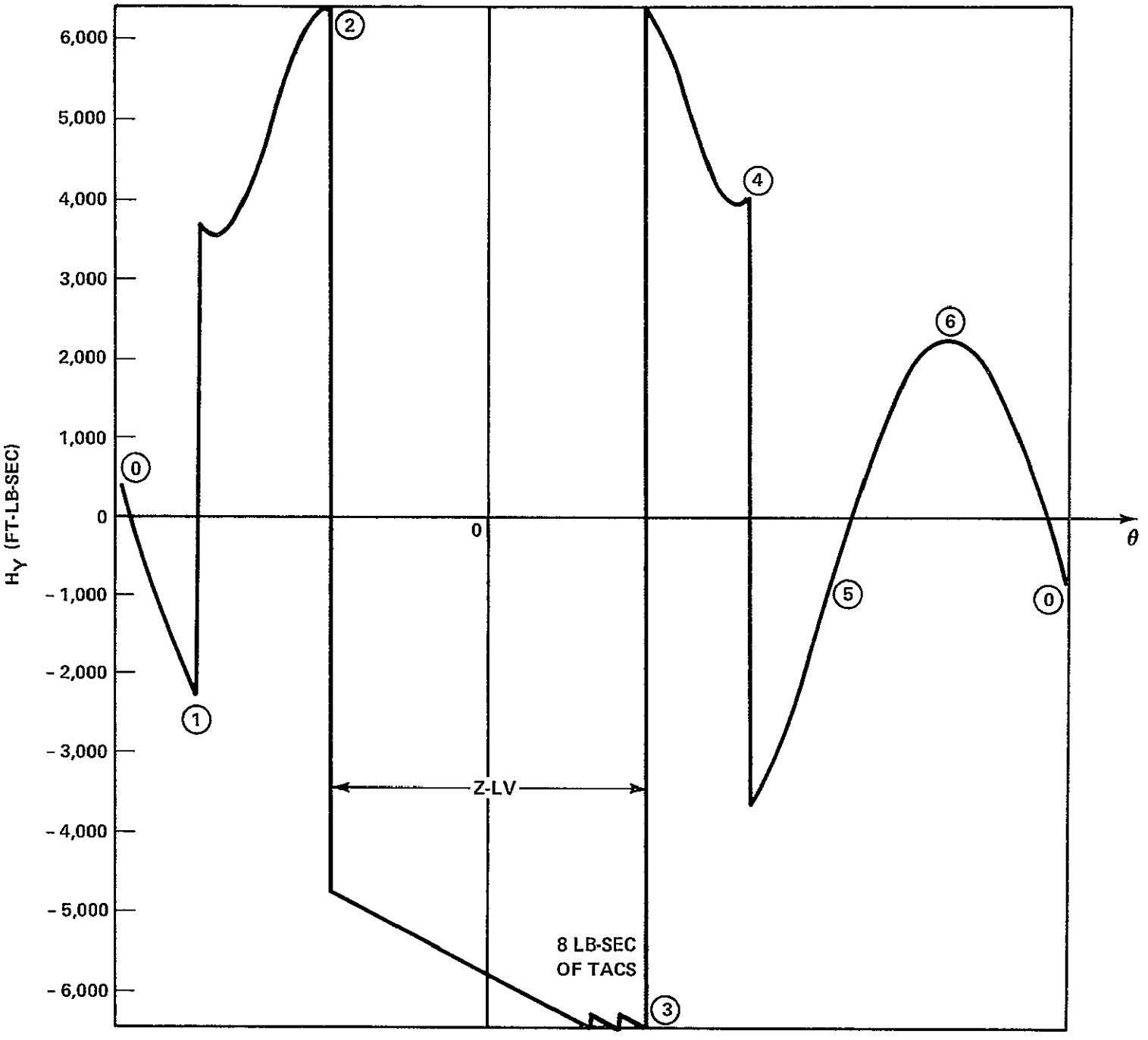

FIGURE 7 - Y-AXIS COMPONENT OF $\underline{H}$ VS ORBITAL ANGULAR EXCURSION, θ.

120° SYMMETRICAL Z-LV PASS, $\beta = 0°$

$\underline{H}'$ (0) = [0 0 0] = $\underline{H}'(\theta_0)$, 2250 FT-LB-SEC PER CMG

SPACECRAFT IN SOLAR INERTIAL FROM (5) TO (0)

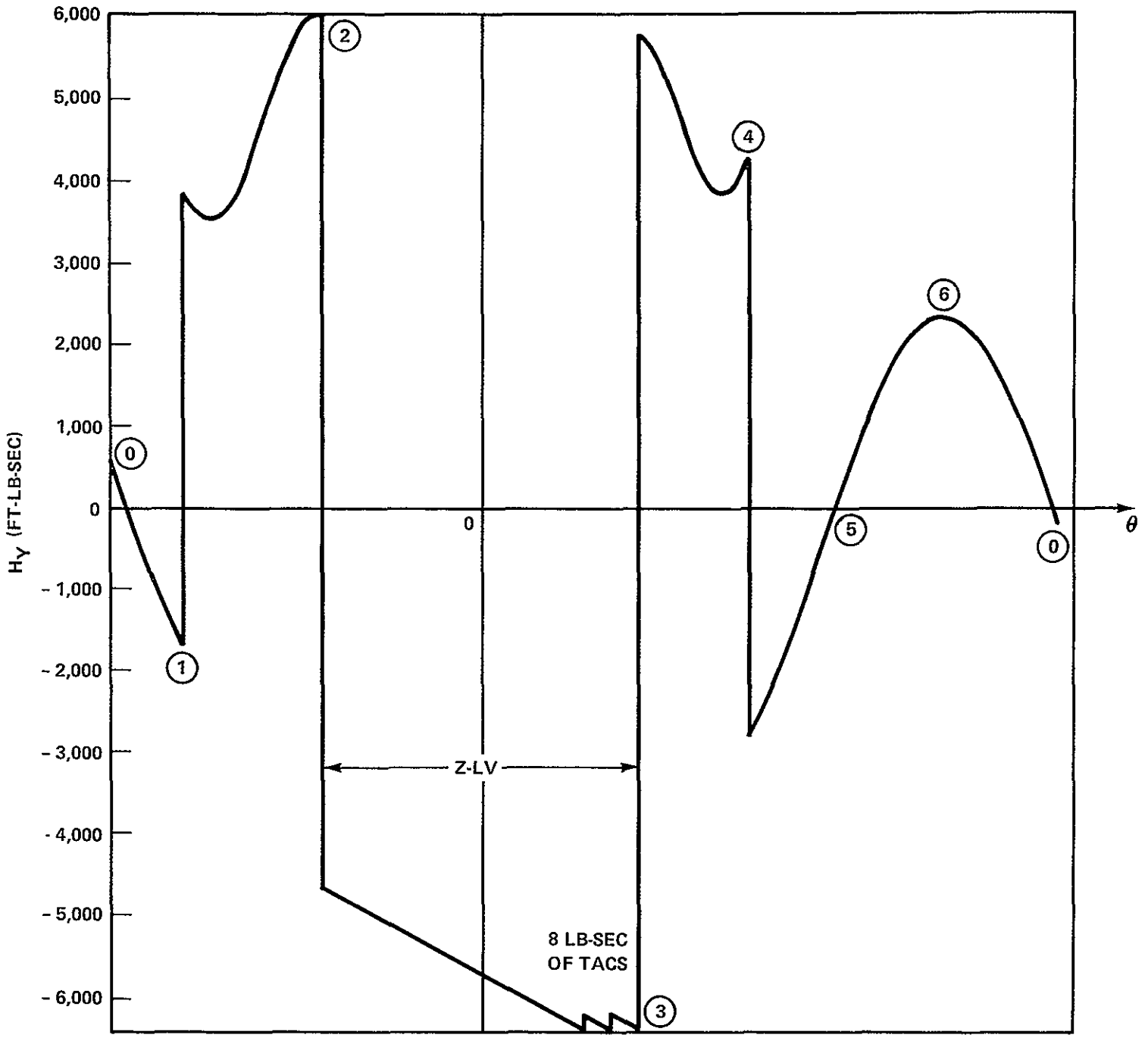

FIGURE 8 – Y-AXIS COMPONENT OF $\underline{H}$ VS ORBITAL ANGULAR EXCURSION, θ.

120° SYMMETRICAL Z-LV PASS, $\beta = 30°$

$\underline{H}'(0) = [\,0\ 0\ 0\,] = \underline{H}'(\theta_0)$, 2250 FT-LB-SEC PER CMG

SPACECRAFT IN SOLAR INERTIAL FROM (5) TO (0)

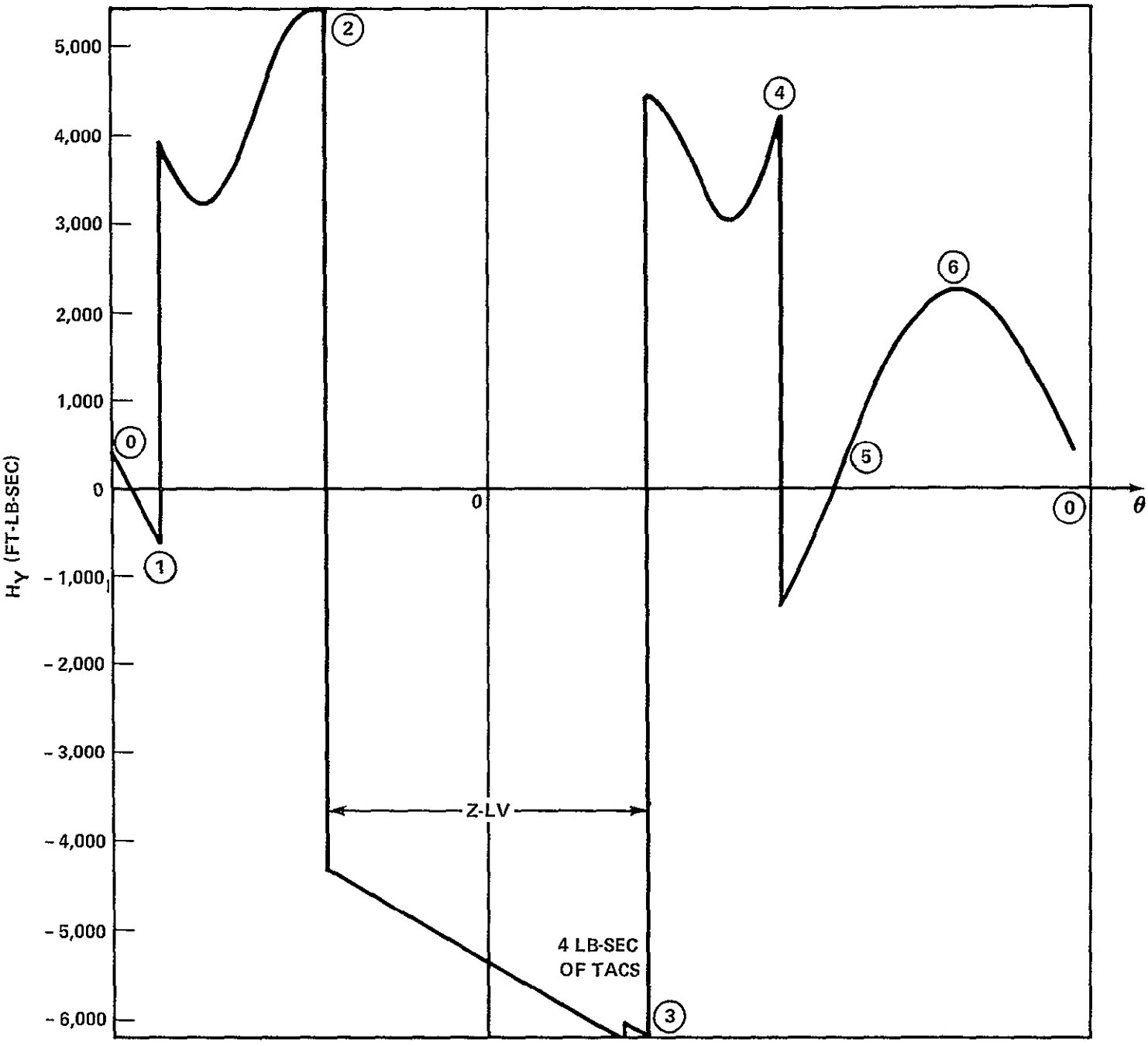

FIGURE 9 - Y-AXIS COMPONENT OF $\underline{H}$ VS ORBITAL ANGULAR EXCURSION, θ

120° SYMMETRICAL Z-LV PASS, $\beta = 50°$
$\underline{H}'$ (⓪) = [0 0 0] = $\underline{H}'(\theta_0)$, 2250 FT-LB-SEC PER CMG
SPACECRAFT IN SOLAR INERTIAL FROM ⑤ TO ⓪

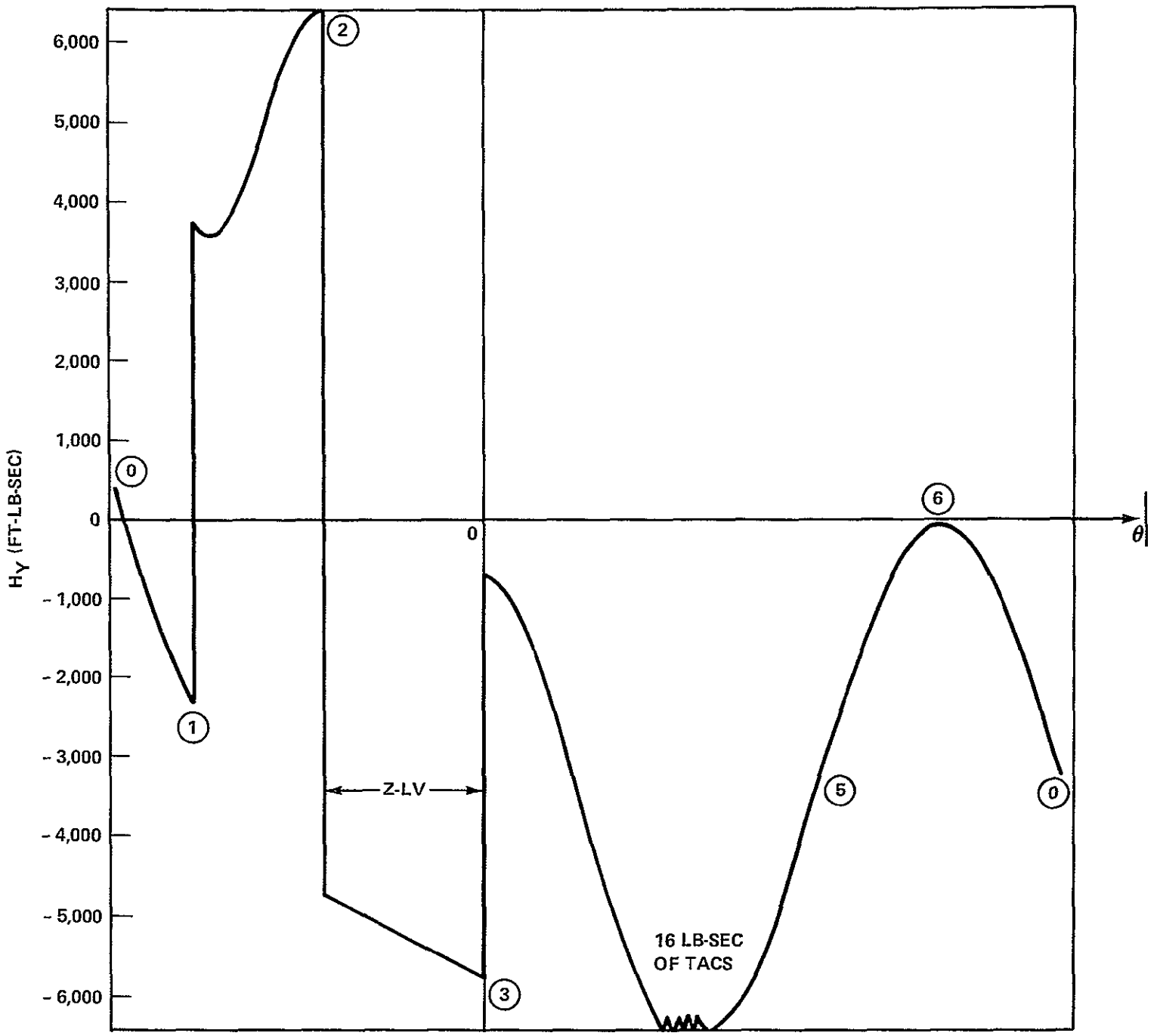

FIGURE 10 - Y-AXIS COMPONENT OF $\underline{H}$ VS ORBITAL ANGULAR EXCURSION, θ.

120° SYMMETRICAL Z-LV PASS, $\beta = 0°$

$\underline{H}'$ (⓪) = [0 0 0] = $\underline{H}'(\theta_0)$, 2250 FT-LB-SEC PER CMG

SPACECRAFT IN SOLAR INERTIAL FROM ⑤ TO ⓪

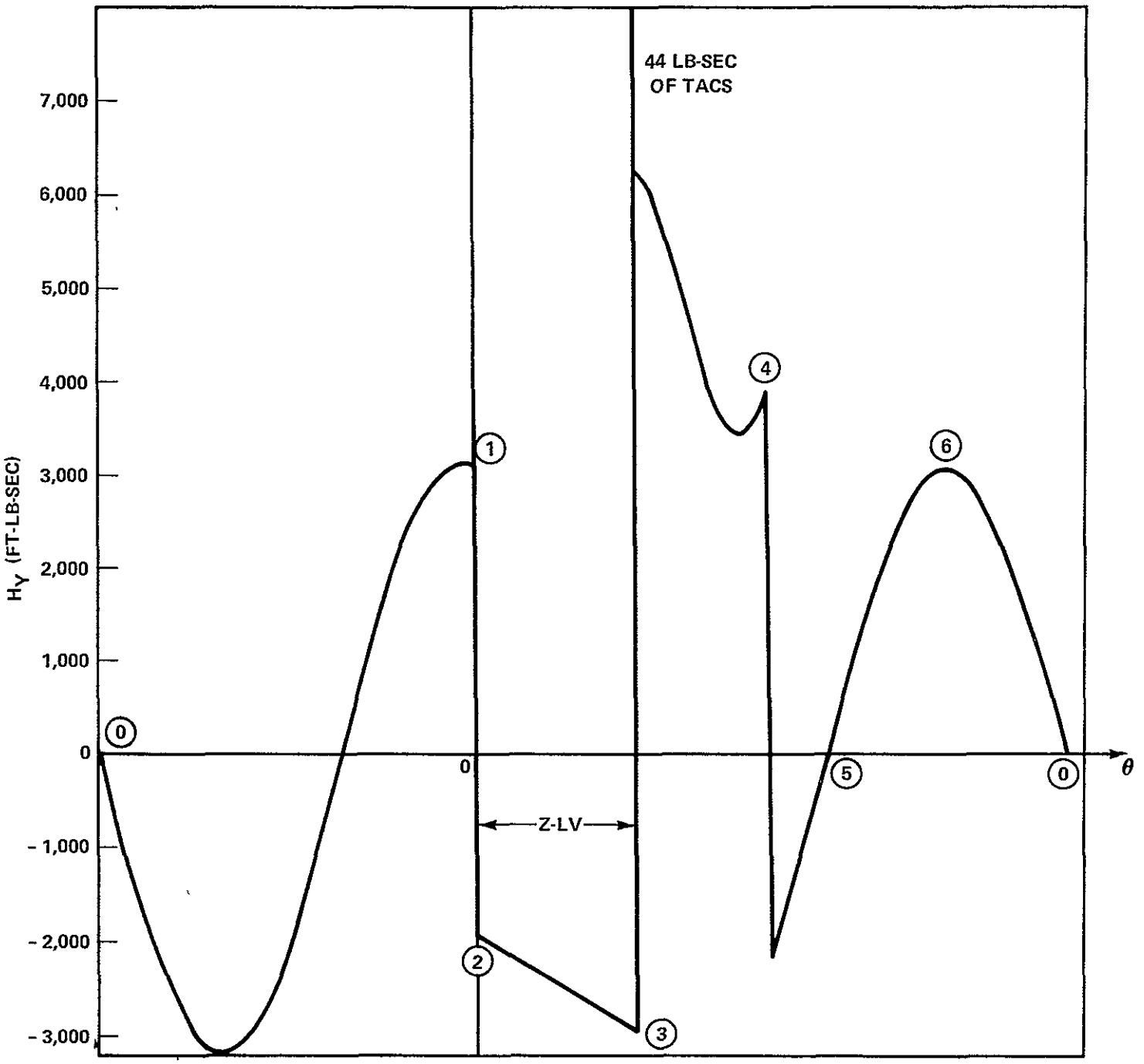

FIGURE 11 - Y-AXIS COMPONENT OF $\underline{H}$ VS ORBITAL ANGULAR EXCURSION, θ.
60° UNSYMMETRICAL Z-LV PASS (NOON ACQUISITION)
$\underline{H}'$ (0) = [0 0 0] = $\underline{H}'(\theta_0)$, 2250 FT-LB-SEC PER CMG
SPACECRAFT IN SOLAR INERTIAL FROM (5) TO (0)

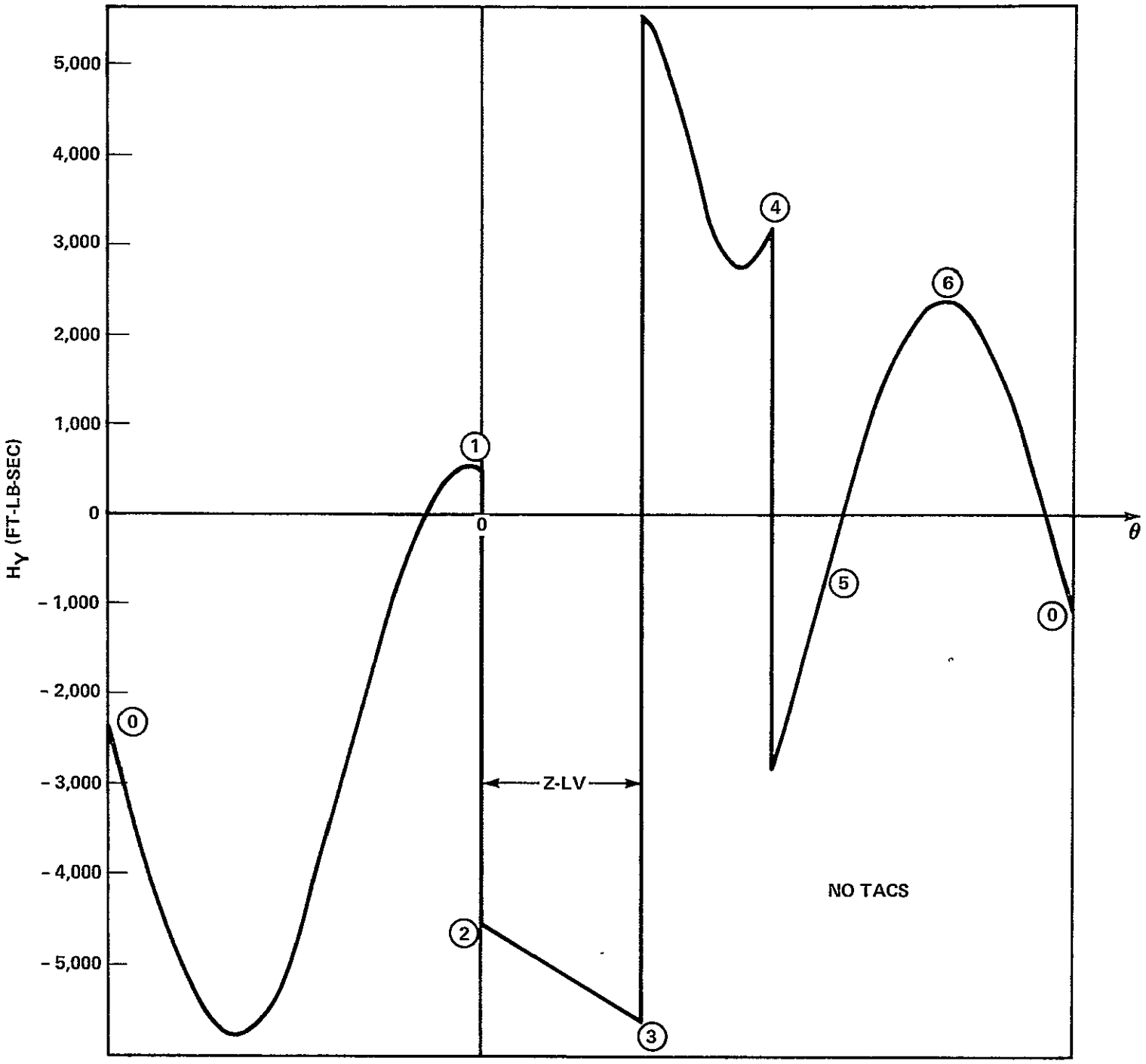

FIGURE 12 – Y-AXIS COMPONENT OF $\underline{H}$ VS ORBITAL ANGULAR EXCURSION, θ.

60^{o} UNSYMMETRICAL Z-LV PASS (NOON ACQUISITION)

$\underline{H}'(⓪) = [\,0\ 0\ 0\,] = \underline{H}'(\theta_0)$, 2250 FT-LB-SEC PER CMG

SPACECRAFT IN SOLAR INERTIAL FROM ⑤ TO ⓪